

**THERMAL PERFORMANCE OF COMPUTER
MICRO-PROCESSOR USING MICROCHANNEL
HEAT SINK WITH NANOFUIDS**

TONY TAN HIN JOO

UNIVERSITI SAINS MALAYSIA

2016

**THERMAL PERFORMANCE OF COMPUTER MICRO-PROCESSOR USING
MICROCHANNEL HEAT SINK WITH NANOFUIDS**

by

TONY TAN HIN JOO

**Thesis submitted in fulfilment of the
requirements for the degree of
Doctor of Philosophy**

December 2016

ACKNOWLEDGEMENTS

Herein I would like to express my greatest appreciation to main my supervisor, Prof. Dr. Zulkifly bin Abdullah, who has given me the most valuable guidance and advices in guiding me to carry out my research work. With his wide professional experience in research work, I have most of the necessary knowledge and skill to be applied in my research systematically and successfully in terms of research methods. Besides this, I also very appreciate his helping effort / advice in necessary arrangement in terms of finance support and tool-equipments preparation that enable me to continuously implement my research professionally.

Herewith I also would like to express my greatest gratitude to my 2nd supervisor, Prof. Dr. Hazizan bin Md. Akil, for his guidance and supporting me in research, especially for the nanofluidic project. Under his guidance, I obtain a lot of knowledge about the nano-materials which is required in my research. Furthermore, the supply of necessary materials and technical advice on the usage of available facilities in laboratory of Material Engineering School are also given to ensure my research can go on smoothly. Besides my supervisors in guiding me in research, I also won't miss out my colleagues, Mr. Khor Chu Yee, Mr. Leong Wei Chiat, Mr. Lau Chun Sean, Mr. Dadan Ramdan, Mr. Muhammad and Khalil Abdullah @ Harun, who have supported and helped me in my research work. Furthermore, I would like to thank Institute of Postgraduate Student (Universiti Sains Malaysia) for financial support in the program of Fellowship along my research work.

Finally, I also won't forget the support and encouragement that have been given from all of my family members along the period of my research work, especially my father, mother and my wife Goh Min Li, and I am very appreciate them.

Tony Tan Hin Joo (December 2016)

TABLE OF CONTENTS

ACKNOWLEDGEMENTS	ii	
TABLE OF CONTENTS	iii	
LIST OF TABLES	vi	
LIST OF FIGURES	vii	
LIST OF SYMBOLS	xvi	
LIST OF ABBREVIATIONS	xvii	
ABSTRAK	xviii	
ABSTRACT	xx	
CHAPTER ONE: INTRODUCTION		
1.1	Introduction	1
1.2	Problem Statement	2
1.3	Objectives of the study	6
1.4	Scope of research work	6
1.5	Thesis outline	8
CHAPTER TWO: LITERATURE REVIEW		
2.1	Introduction	10
2.2	Study on the effect of fluid flow, various microchannel heat sink configurations and physical channel dimensions	10
2.3	Study on the effect of nanofluid in cooling performance of microchannel heat sink	24
2.4	Summary	34

CHAPTER THREE – METHODOLOGY

3.1	Introduction	37
3.2	Development of Model	38
3.2.1	Equation solution for modelling	40
3.2.2	Development of mesh modelling	42
3.2.3	Boundary conditions	43
3.2.4	Grid independency	44
3.3	Experiment setup	45
3.3.1	Equipment setup	45
3.3.2	Nanofluids preparation	51
3.4	Work flow of experimental and simulation analysis	53
3.5	Summary	58

CHAPTER FOUR – RESULT AND DISCUSSION

4.1	Introduction	59
4.2	Validation of simulation work through experimental work	60
4.3	Analysis of the effect of various geometrical configurations of microchannels on the heat sink performances	67
4.4	Analysis of performance of microchannel by considering the effect of nanofluid on the heat sink performances	76
4.5	Analysis of performance of microchannel by considering the effect of nanofluid concentrations	81
4.6	Analysis of performance of microchannel by considering the effect of nanofluid types	85
4.7	Analysis of the effect of vertical and horizontal fin-tip gaps for the various geometrical configurations of microchannels	91

4.8	Analysis of the effects of geometry and number of hollow on the performance of microchannel heat sinks	101
-----	--	-----

CHAPTER FIVE – CONCLUSION

5.1	Conclusion	110
5.2	The effects of various geometrical configurations of microchannel on heat sink performance	110
5.3	The effect of nanofluid on the performance of microchannel heat sink	111
5.4	The effect of nanoparticle concentration of nanofluid on the performance of microchannel heat sink	111
5.5	The effect of nanoparticles types of nanofluid on the performance of microchannel heat sink	112
5.6	The effect of vertical and horizontal fin tip gaps on the performance of microchannel heat sinks	112
5.7	The effect of geometry and number of hollow on the performance of microchannel heat sinks	113
5.8	Recommendation for future works	113

REFERENCES	115
-------------------	------------

LIST OF PUBLICATIONS

LIST OF TABLES

		Page
Table 1	Comparison of experimental result with simulation result at various grid sizes.	45

LIST OF FIGURES

	Page
Figure 1.1 Computer processor cooling by heat sink with the application of fan.	2
Figure 1.2 Heat pipe with fins for cooling.	2
Figure 1.3 Various configurations of heat sink fin geometry.	3
Figure 1.4 Heat sink using liquid medium for cooling in computer CPU.	4
Figure 1.5 Microchannel heat sink.	5
Figure 2.1 Geometric configurations of N-, S-, D-, U-, and V-type arrangement of inlet and outlet of microchannel heat sink.	11
Figure 2.2 Schematic of microchannel configurations of (a)square and rectangular channels, (b)circular channels, (c)trapezoidal channels, (d)triangular channels.	13
Figure 2.3 Schematic of microchannel heat sink with fin tip clearance.	14
Figure 2.4 (a)Shrouded array geometry, (b)pin fin with tip clearance, and (c)pin fin without tip clearance.	15
Figure 2.5 (a)Test module, (b)Microchannel heat sink.	16
Figure 2.6 Experimental set-up.	17
Figure 2.7 Schematic diagram of the liquid cooling concept for electronic packages.	18
Figure 2.8 Cross-sectional view of the microchannel heat sink on the flip chip ball grid array packages.	18
Figure 2.9 Schematic diagram of the test section and microchannel heat sink.	19

Figure 2.10	Schematic of the microchannel heat sink: (a)system, (b)microscope image of silicon microchannels, (c)geometric shape of microchannel.	20
Figure 2.11	Structure of rectangular microchannel heat sink.	21
Figure 2.12	Structure and size of heat sinks: (a)structure, (b)size, (c)packaging.	22
Figure 2.13	Schematic of the (a)two-layered MCHS and (b)a repeated section of MCHS.	23
Figure 2.14	The schematic of the heat sink: (a)new design with truncated top channels (b)original design.	24
Figure 2.15	(a)Schematic diagram of computational domain, (b)Cross section of rectangular shaped microchannel.	28
Figure 2.16	(a)Schematic diagram of computational domain, (b)Cross section of trapezoidal shaped microchannel.	29
Figure 2.17	Schematic diagram of computational domain, (a)isometric view of microchannel heat exchanger, (b)cross sectional view of microchannel heat exchanger.	30
Figure 2.18	(a)3D view, (b)top view, (c)side view of the single IMCHS.	32
Figure 3.1	Flow chart of microchannel heat sink model development for simulation analysis.	39
Figure 3.2	Meshing work for various geometrical configurations of microchannels.	42
Figure 3.3	Boundary condition for the 3D modeling of microchannel heat sinks.	43
Figure 3.4	General view of experimental setup.	45
Figure 3.5	Assembly of microchannel heat sink.	46

Figure 3.6	Schematic diagram of equipment system for experimental work.	47
Figure 3.7	(a)rectangular-, (b)triangular-, and (c)trapezoidal microchannel heat sinks.	48
Figure 3.8	Assembly arrangement of microchannel heat sinks with casings and heaters.	50
Figure 3.9	Cross-sectional view of assembly of microchannel heat sink with casings and heaters.	51
Figure 3.10	Comparison of 3% concentration of nanoparticles within nanofluids ($\text{SiO}_2\text{-H}_2\text{O}$ and $\text{Al}_2\text{O}_3\text{-H}_2\text{O}$) with- and without settlement of nanoparticles.	52
Figure 3.11	Geometrical configuration dimensions of microchannel heat sink (all dimensions in mm).	54
Figure 3.12	Dimensions of cross sectional microchannel heat sink (all dimensions in mm) and schematic diagram of various fin configurations without and with vertical fin tip gap.	54
Figure 3.13	Semi - hollow fin and fully closed hollow channels at optimum vertical fin tip gap condition in microchannel heat sink.	55
Figure 3.14	The microchannel heat sink model with dimensions (in mm).	56
Figure 3.15	The cross sectional side view of the heat sink showing the channels (M1 to M11) and fins (H1 to H10), and the dimensions (in mm).	56
Figure 3.16	Solid fin and fins with various hollow geometries.	57
Figure 4.1	Pressure drop within rectangular microchannel heat sink with distilled water.	60

Figure 4.2	Pressure drop within triangular microchannel heat sink with distilled water.	61
Figure 4.3	Pressure drop within trapezoidal microchannel heat sink with distilled water.	61
Figure 4.4	Pumping power for the fluid flow through rectangular microchannel heat sink with distilled water.	62
Figure 4.5	Pumping power for the fluid flow through triangular microchannel heat sink with distilled water.	62
Figure 4.6	Pumping power for the fluid flow through trapezoidal microchannel heat sink with distilled water.	63
Figure 4.7	Heat sink base temperature for rectangular microchannel heat sink with distilled water.	64
Figure 4.8	Heat sink base temperature for triangular microchannel heat sink with distilled water.	64
Figure 4.9	Heat sink base temperature for trapezoidal microchannel heat sink with distilled water.	65
Figure 4.10	Thermal resistance for rectangular microchannel heat sink with distilled water.	66
Figure 4.11	Thermal resistance for triangular microchannel heat sink with distilled water.	66
Figure 4.12	Thermal resistance for trapezoidal microchannel heat sink with distilled water.	67
Figure 4.13	Comparison of pressure drop among various geometrical configurations of microchannels with distilled water, by simulation work.	68

Figure 4.14	Comparison of pumping power among various geometrical configurations of microchannels with distilled water, by simulation work.	69
Figure 4.15	Comparison of heat sink base temperature among various geometrical configurations of microchannels with distilled water, by simulation work.	70
Figure 4.16	Comparison of heat transfer coefficient among various geometrical configurations of microchannels with distilled water, by simulation work.	71
Figure 4.17	Comparison of thermal resistance among various geometrical configurations of microchannels with distilled water, by simulation work.	72
Figure 4.18	Comparison of performance index among various geometrical configurations of microchannels with distilled water, by simulation work.	72
Figure 4.19	Velocity and temperature contour for various geometrical configurations of microchannel heat sinks with distilled water as cooling medium at fluid flow velocity of 0.0298 m/s.	74
Figure 4.20	Pressure drop within rectangular microchannel heat sink with alumina nanofluids with 1% concentration.	77
Figure 4.21	Pumping power for the fluid flow through rectangular microchannel heat sink with alumina nanofluids with 1% concentration.	78
Figure 4.22	Heat sink base temperature for rectangular microchannel heat sink with alumina nanofluids with 1% concentration.	79

Figure 4.23	Heat transfer coefficient for rectangular microchannel heat sink with alumina nanofluids with 1% concentration.	79
Figure 4.24	Thermal resistance for rectangular microchannel heat sink with alumina nanofluid with 1% concentration.	80
Figure 4.25	Pressure drop within rectangular microchannel heat sink with alumina nanofluids with 1%, 2% and 3% concentrations, by simulation work.	82
Figure 4.26	Pumping power for the fluid flow through rectangular microchannel heat sink with alumina nanofluids with 1%, 2% and 3% concentrations, by simulation work.	82
Figure 4.27	Heat sink base temperature for rectangular microchannel heat sink with alumina nanofluids with 1%, 2% and 3% concentrations, by simulation work.	83
Figure 4.28	Heat transfer coefficient for rectangular microchannel heat sink with alumina nanofluids with 1%, 2% and 3% concentrations, by simulation work.	84
Figure 4.29	Thermal resistance for rectangular microchannel heat sink with alumina nanofluids with 1%, 2% and 3% concentrations, by simulation work.	85
Figure 4.30	Comparison of pressure drop among various types of nanofluids within rectangular microchannel at 3% concentration of nanoparticles, by simulation work.	86
Figure 4.31	Comparison of pumping power among various types of nanofluids within rectangular microchannel at 3% concentration of nanoparticles, by simulation work.	87

Figure 4.32	Comparison of heat sink base temperature among various types of nanofluids within rectangular microchannel at 3% concentration of nanoparticles, by simulation work.	88
Figure 4.33	Comparison of heat transfer coefficient among various types of nanofluids within rectangular microchannel at 3% concentration of nanoparticles, by simulation work.	89
Figure 4.34	Comparison of thermal resistance among various types of nanofluids within rectangular microchannel at 3% concentration of nanoparticles, by simulation work.	90
Figure 4.35	Comparison of temperature contour for microchannel heat sink with silica and alumina nanofluids (3% concentration) as cooling medium at fluid flow velocity of 0.0298 m/s.	91
Figure 4.36	Pressure drop comparison as function of vertical fin tip gap, among various fin configurations of microchannel heat sink at volume flow rate of $6.8 \times 10^{-7} \text{ m}^3/\text{s}$.	92
Figure 4.37	Total thermal resistance comparison as function of vertical fin tip gap, among various fin configurations of microchannel heat sink at volume flow rate of $6.8 \times 10^{-7} \text{ m}^3/\text{s}$ and heat flux of $300000 \text{ W}/\text{m}^2$.	93
Figure 4.38	Convective area of various fin configurations of microchannel heat sink.	94
Figure 4.39	Introduction of new convective area as the vertical fin tip gap is introduced.	94
Figure 4.40	Figure 4.40: Velocity distribution in 6 th rectangular channel and in the vertical fin tip gap above 5 th rectangular fin at volume flow rate of $6.8 \times 10^{-7} \text{ m}^3/\text{s}$.	96

Figure 4.41	Maximum heat sink base temperature as function of vertical fin tip gap, among various fin configurations of microchannel heat sink at volume flow rate of $6.8 \times 10^{-7} \text{ m}^3/\text{s}$ and heat flux of 300000 W/m^2 .	97
Figure 4.42	Temperature contour of heat sink base for various fin configurations of microchannel heat sink at vertical fin tip gap of 0.08mm , volume flow rate of $6.8 \times 10^{-7} \text{ m}^3/\text{s}$ and heat flux of 300000 W/m^2 .	98
Figure 4.43	Introduction of horizontal fin convective area as the horizontal fin tip gap decreases.	99
Figure 4.44	Pressure drop as function of different horizontal fin tip gap in microchannel heat sink with optimum vertical fin tip conditions at volume flow rate of $6.8 \times 10^{-7} \text{ m}^3/\text{s}$.	100
Figure 4.45	Total thermal resistance as function of different horizontal fin tip gap in microchannel heat sink with optimum vertical fin tip conditions at volume flow rate of $6.8 \times 10^{-7} \text{ m}^3/\text{s}$ and heat flux of 300000 W/m^2 .	101
Figure 4.46	Comparison of velocity distributions of fluid flow across the channels and hollows among cases A, B1, C1 and D1.	102
Figure 4.47	Comparison of velocity distributions between channel (M6) and hollow (H5).	103
Figure 4.48	Comparison of pressure drop across the heat sink for cases with solid fin and single-hollow fins.	103
Figure 4.49	Temperature contour of heat sink structure with solid and single-hollow fins at volume flow rate of $1.3 \times 10^{-5} \text{ m}^3/\text{s}$.	104

Figure 4.50	Temperature contour of heat sink base with solid and single-hollow fins at volume flow rate of $1.3 \times 10^{-5} \text{ m}^3/\text{s}$.	105
Figure 4.51	Average temperature of heat sink base with solid and single-hollow fins as function of volume flow rate.	105
Figure 4.52	Comparison of total thermal resistance of heat sink with solid and single-hollow fins, as function of volume flow rate.	106
Figure 4.53	Pressure drop across the heat sink with single and double hollow fins as function of volume flow rate.	107
Figure 4.54	Average heat sink base temperature with single and double hollow fins as function of volume flow rate.	107
Figure 4.55	Temperature contours of heat sink base with single and double hollow fins at volume flow rate of $1.3 \times 10^{-5} \text{ m}^3/\text{s}$.	108
Figure 4.56	Total thermal resistance of heat sink with single and double hollow fins as function of volume flow rate.	109

LIST OF SYMBOLS

u	Fluid flow velocity component in x-direction
v	Fluid flow velocity component in y-direction
w	Fluid flow velocity component in z-direction
P	Pressure
x, y, z	Cartesian coordinates
T	Temperature
k	Thermal conductivity
c_p	Specific heat capacity
Re	Reynolds Number
h	Heat transfer coefficient
ρ	Density
μ	Dynamic viscosity
φ	Volume fraction of nanoparticle
R	Thermal resistance
ΔT	Temperature difference
Q	Heat input
Q_f	Flow rate
ΔP	Pressure difference
P_{pump}	Pumping power
q	Heat transfer

LIST OF ABBREVIATIONS

FVM	Finite Volume Method
IMCHS	Interrupted Microchannel Heat Sink
MCHS	Mircochannel Heat Sink
3-D	Three-Dimensional

**PRESTASI THERMA DALAM MIKRO-PEMPROSESAN KOMPUTER
DENGAN MENGGUNAKAN NANOFLUID DALAM MIKRO PENYERAP
HABA**

ABSTRAK

Dalam perkembangan teknologi elektronik yang pesat, permintaan terhadap komputer berkapasiti tinggi semakin meningkat setiap tahun. Apabila kapasiti komputer semakin meningkat, haba yang dihasilkan daripada komponen pemprosesan semakin meningkat semasa berfungsi. Dengan ketiadaan pengurusan haba yang sesuai, haba tinggi yang dihasilkan tersebut akan menyebabkan suhu tinggi pada komponen pemprosesan komputer dan akibatnya prestasi komputer akan menurun sehingga pada akhirnya komponen akan mengalami kerosakan. Pada masa yang sama, proses pengecilan saiz komponen elektronik yang berterusan itu menyumbang kesan impak terhadap saiz sistem penyejukan yang dihubungkan kepada komponen pemprosesan komputer tersebut. Secara amnya, dalam teknologi sistem penyejukan yang sedia ada, saiz sistem penyejukan konvensional telah digunakan dalam pasaran and pelbagai jenis medium penyejukan digunakan untuk menyerap dan membebaskan haba. Walaubagaimanapun, kapasiti penyejukan bagi sistem penyejukan konvensional tersebut adalah terhad dan tidak mampu mengeluarkan haba tinggi daripada komponen pemprosesan komputer yang berkapasiti tinggi. Selain itu, saiz yang besar tidak dapat dimuatkan ke atas komponen pemprosesan komputer yang semakin kecil. Dengan itu, langkah - langkah yang sesuai untuk menangani masalah pengurusan haba yang tinggi dan fizikal saiz yang kecil bagi sistem penyejukan adalah diperlukan. Sebagai penyelesaiannya, mikro penyerap haba telah diperkenalkan. Dalam penyelidikan tersebut, pelbagai parameter (hilang tekanan [range: 20Pa – 38Pa], suhu [range: 342K – 354K] and Reynolds Number [range: 70 – 1150]), fizikal dimensi dan bentuk saluran penyerap haba (segi empat panjang, tiga segi dan trapezoid) telah dipertimbangkan and

dianalisis terhadap impaknya ke atas prestasi mikro penyerap haba. Penyelidikan tersebut telah dijalankan melalui kaedah simulasi. Dalam kaedah eksperimen, pelbagai medium penyejukan digunakan iaitu air penyulingan dan nanofluid (air penyulingan + alumina Al_2O_3 , dan air penyulingan + silica SiO_2) dengan kandungan zarah-zarah nano yang berlainan (1%, 2% and 3% kandungan). Manakala dalam kaedah simulasi, komputer pengisian FLUENT berdasarkan Finite Volume Method (FVM) telah digunakan untuk menyimulasikan keupayaan mikro penyerap haba. Keputusan kajian tersebut menunjukkan bahawa faktor fizikal dimensi dan bentuk memberikan kesan impak yang tinggi terhadap prestasi haba bagi mikro penyerap haba. Dengan itu, saluran berbentuk segi empat panjang mampu memindahkan haba yang tinggi berbanding dengan bentuk saluran mikro yang lain, tetapi ia menunjukkan prestasi hidrodinamik yang rendah. Sebaliknya, mikro saluran segi tiga menunjukkan prestasi pemindahan haba yang rendah walaupun prestasi hidrodinamik yang tinggi. Analisis terhadap kesan jenis zarah – zarah nano (Al_2O_3 dan SiO_2) dan kandungannya (1%, 2% dan 3% kandungan) dalam asas medium penyejukan ke atas prestasi mikro penyerap haba telah dijalankan dalam kajian tersebut. Hasil analisis tersebut menunjukkan bahawa kehadiran zarah – zarah nano dalam asas medium penyejukan dapat meningkatkan prestasi penyejukan sebanyak 40% berbanding dengan penggunaan air penyulingan sahaja. Manakala dengan peningkatan kandungan zarah – zarah nano dalam asas medium penyejukan, kadar penyejukan meningkat. Walaubagaimanapun, kuantiti kandungan zarah – zarah nano yang rendah tidak mempengaruhi prestasi hidrodinamik bagi mikro penyerap haba. Sebagai kesimpulannya, kesan fizikal dimensi, bentuk saluran mikro dan kehadiran zarah – zarah nano dalam asas medium penyejukan merupakan faktor – faktor penting dan menunjukkan impaknya yang jelas ke atas prestasi saluran mikro penyerap haba. Bagi menunjukkan keputusan simulasi yang dihasilkan itu menyakinkan, kaedah eksperimen telah dijalankan bagi mengesahkan keputusan tersebut.

THERMAL PERFORMANCE OF COMPUTER MICRO-PROCESSOR USING MICROCHANNEL HEAT SINK WITH NANOFLUIDS

ABSTRACT

In the rapid development of electronic technology, the demand of high capacity in computer performance is increasing every year. The higher the performance of computer the higher the heat will be released from the computer processor. Without proper management of the heat release, the generated high heat will cause computer performance deteriorate due to high temperature and may cause damage consequently. Furthermore, the continuous miniaturization process of electronic component has contributed impact to the size of cooling system which is incorporated with the electronic component. As commonly found in the current technology of cooling system, the conventional size of cooling system is used, and various medium are applied through the cooling system for heat removal purpose. The heat removal capacity of conventional cooling system is limited which is not able to dispel the high heat that generated from high performance computer processor. Furthermore, the larger size of the conventional cooling system can not be fitted into the smaller size of electronic components of the processor. As a result, a proper approach of managing the high heat issue and proper physical size of cooling system is required, in which microchannel heat sink is introduced. In the research work, various operating conditions (pressure drop [range: 20Pa – 38Pa], temperature [range: 342K – 354K] and Reynolds Number [range: 70 – 1150]), physical dimensions and channel configurations (rectangular, triangular and trapezoidal) are considered and analysed in order to investigate their impact on the microchannel heat sink performance in terms of pressure drop, pumping power, thermal resistance, and heat transfer coefficient. Besides this, various cooling working medium has been used such as distilled water and nanofluid (Distilled Water H₂O + Alumina

Al_2O_3 and Distilled Water H_2O + Silica SiO_2) with various concentrations of nanoparticles (1%, 2% and 3% concentration). Simulation work by applying Finite Volume Method (FVM) in FLUENT software has been carried out to simulate the engineering results for the performance of microchannel heat sink. It is found that the physical dimension and geometrical channel configuration have obvious impact on the microchannel heat sink performance in which the case of rectangular channel that provides the highest heat transfer performance. Besides this, the research work also shows that the effect of different types and concentrations (1%, 2% and 3% concentrations) of nanoparticles within cooling medium plays important role onto the microchannel heat sink performance. The increment of cooling performance by 40% can be achieved by adding nanoparticles into cooling medium as compared with pure distilled water. Furthermore, the increment of cooling rate also can be achieved by the increment of nanoparticles concentration. In the research work, nanofluid Alumina provides the higher cooling rate as compare with pure distilled water and nanofluid Silica due to the effect of high thermal conductivity. However, the small amount of nanoparticles concentration would not affect hydrodynamic performance of microchannel heat sink. As a result, the physical dimension, channel geometrical configurations, existence of nanoparticles within cooling medium are vital factors that able to affect and incur obvious impact on the performances of microchannel heat sink hydrodynamically and thermally. To ensure the result of the simulation work above is reliable, the experimental works have been carried out for validation and comparison.

CHAPTER ONE

INTRODUCTION

1.1 Introduction

Cooling is a very important process in removing the generated heat from an equipment, like electronic components, air-conditioning systems, engine, fuel cells, etc. Without cooling process, the successive generated heat will cause high temperature and the high temperature effect will then causes deterioration in performance and may damage seriously. In order to overcome the high temperature that generated from heat, the cooling process is required. There are various cooling equipments are available in industrial technology such as heat exchanger systems, heat pipe, radiator, condenser, and heat sink. Figures 1.1 and 1.2 show the examples of cooling equipment for electronic component. In conjunction with the use of these cooling equipments, there are various types of working medium are used in these cooling equipments, such as air, water, R-12, R-113, R-141b, R-124, R-134a, ethanol, etc, as coolant to absorb and transport the heat for removal.

In electronic industries for computer technology, cooling process for the electronic components is vital in order to maintain their high performance in function and prevent any damage that caused by the high temperature effect. For instant, microprocessor in CPU (Central Processing Unit) of the high performance computer system. The study of fluid flow and heat transfer for cooling process of the processor has been carried out substantially by various researchers around the world. However, there is still having several issues which have not been investigated. Hence, the related issues have been identified and studied in this research as complimentary for the previous research works, and finally reported / documented in the following chapter in this thesis.

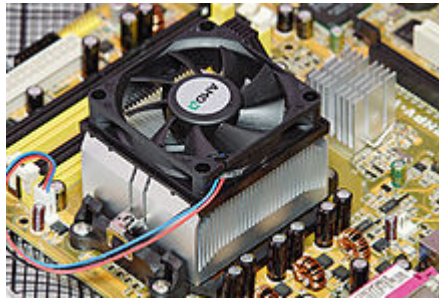
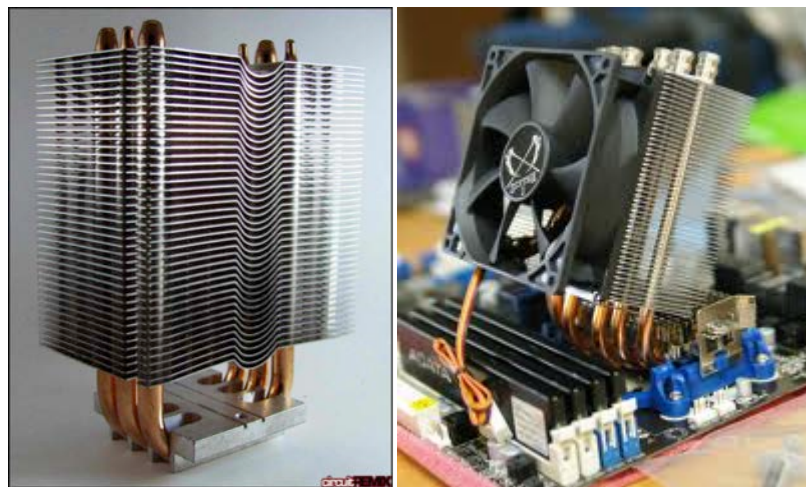


Figure 1.1: Computer processor cooling by heat sink with the application of fan.

(Source:

https://en.wikipedia.org/wiki/Computer_cooling#/media/File:AMD_heatsink_and_fan.jpg)



(a)

(b)

Figure 1.2: Heat pipe with fins for cooling.

(Source: Figure (a)-<http://liquid-cooling.org/wp-content/uploads/2014/05/Figure-9-Sample-heat-sink-with-heat-pipe-Source-circuitremix.com-.png>,

Figure (b)-

https://en.wikipedia.org/wiki/Computer_cooling#/media/File:Heatsink_with_heat_pipes.jpg)

1.2 Problem Statement

As can be seen in the available cooling heat sink design, various configuration of fin has been designed to suit specific engineering application as shown in Figures 1.3. The example of heat sink assembly onto computer CPU board is also shown in Figure 1.3(e).